The Thickness Distribution of Sea Ice

A. S. THORNDIKE, D. A. ROTHROCK, G. A. MAYKUT, AND R. COLONY

University of Washington, Seattle, Washington 98195

The polar oceans contain sea ice of many thicknesses ranging from open water to thick pressure ridges. Since many of the physical properties of the ice depend upon its thickness, it is natural to expect its large-scale geophysical properties to depend on the relative abundance of the various ice types. The ice pack is treated as a mixture whose constituents are determined by their thickness and whose composition is determined by the area covered by each constituent. A dimensionless function $g(h)$, the ice thickness distribution, is defined such that $g(h)\,dh$ is the fraction of a given area covered by ice of thickness greater than h but less than $h + dh$. A theory is developed to explain how the ice thickness distribution changes in response to thermal and mechanical forcing. The theory models the changes in thickness due to melting and freezing and the rearrangement of existing ice to form leads and pressure ridges. In its present form the model assumes as inputs a growth rate function and the velocity field of the ice pack. The model is tested using strain data derived from the positions of three simultaneous manned drifting stations in the central Arctic during the period 1962–1964 and growth rates inferred from climatological heat flux averages. The results are compared with estimates of g based on submarine measurements of ice thickness.

INTRODUCTION

On a geophysical scale the ice pack can be thought of as a mixture of individual constituents which, because of their different thicknesses, respond differently to similar thermal and mechanical forcing. A given region of pack ice may contain open water, young ice centimeters thick, multiyear ice a few meters thick, and pressure ice up to tens of meters thick (Figures 1 and 2). Among the many properties of sea ice strongly dependent upon its thickness are compressive strength, rate of growth, surface temperature, turbulent and radiative heat exchange with the atmosphere, potential energy, and salt content. Consequently, the aggregate properties of the ice pack may be inferred from the properties and relative abundance of each constituent. In the first part of this paper we describe the small-scale processes involved in producing and maintaining ice of different thicknesses, and from these we develop a model to describe the large-scale consequences.

Consider some region **R** in the ice pack with an area R, and with a length scale assumed to be large compared with the typical length scales of ridges, leads, and floes. Let $A(h_1, h_2)$ be the area within **R** covered by ice of thickness h in the range $h_1 \leq h < h_2$; we then define the thickness distribution $g(h)$ by

$$\int_{h_1}^{h_2} g(h)\,dh = \frac{1}{R}A(h_1, h_2) \qquad (1)$$

As we shall discuss later, $g(h)$ is also a function of time and position. While little is known regarding spatial or temporal variations in $g(h)$ in either polar ocean, there is a spatter of data from the central Arctic from which we infer the general form of $g(h)$ in that region. Figure 3, after *LeSchack et al* [1971] and *Swithinbank* [1972], shows thickness distributions calculated from submarine data.

Two phenomena act to alter the thickness of floating ice and, consequently, cause changes in $g(h)$: thermodynamic processes are responsible for mass changes at the upper and lower boundaries of the ice, and mechanical processes, resulting from the nonuniform motion of the ice, cause the formation of leads and pressure ridges. The pack ice observed in the field is vastly different from the ice that would exist if either of these processes were somehow suppressed. If the ice did not deform, for instance, all the ice in a particular climatic region would approach a uniform thickness of thermodynamic equilibrium. If, on the other hand, the thermodynamics were turned off so that there could be no freezing or melting, then eventually all the ice thinner than some critical value would be heaved up into pressure ridges. Assuming that the rubble pile associated with most pressure ridges would remain consolidated, the ice pack would then settle into a steady state consisting of deformed ice and open water. Despite the simplified nature of these examples, they emphasize the critical difference in character between the thermodynamics and the mechanics: on a yearlong average the thermodynamics strives for a single equilibrium thickness by net accretion to the thin ice and net ablation from the thick; in contrast, the mechanics creates both thick pressure ice and open water. The thermodynamics seeks the mean and the mechanics the extremes. The thickness distribution is an historical integral of the continuous and simultaneous action of these two processes.

Except for fast ice near the continental margins the ice pack is in continual motion, driven by the atmosphere and ocean. For reasons not treated here (e.g., thermal cracking and uneven hydrostatic loading) we assume that the ice cover is isotropic and densely fractured. It is able to move and to deform significantly because of concentrated deformations at cracks, rather than by even and continuous deformation throughout. Figure 4 shows time series of divergence and shear on a 1000-km scale in the central Arctic; the values are derived from daily position measurements of three contemporaneous drifting stations, T-3, Arlis 2, and NP-10, over a 2-year period. The data have been smoothed with a time scale of about 1 week to suppress the rather large measurement errors. (To our knowledge, the motions of these and the other 25 or so manned drifting stations are not available in published form. The data have been collected from many sources and are accessible through the office of the Arctic Ice Dynamics Joint Experiment (Aidjex) at the University of Washington, Seattle.) The motion is seen to be generally diverging, the magnitude of the shear being comparable to the divergence. Similar results have been obtained on a 100-km scale over a period of a few months [*Thorndike*, 1974] and on smaller scales by *Hibler et al.* [1974]. These data describe an ice pack that undergoes de-

Copyright © 1975 by the American Geophysical Union.

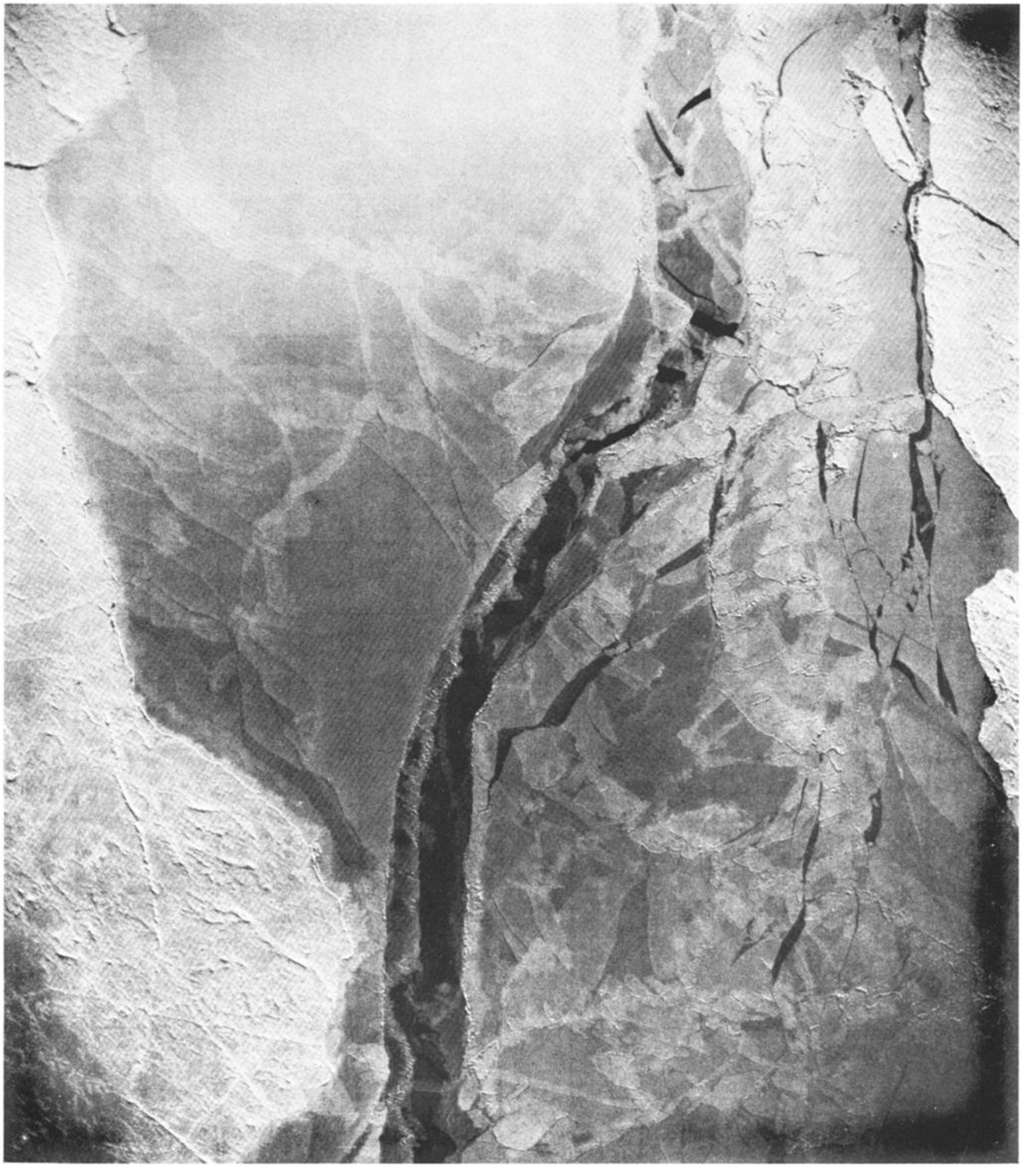

Fig. 1. NAVOCEANO photograph of a region about 15 km across, taken from an altitude of 30,000 ft (9 km) in April 1972. Ice thickness corresponds approximately to the shade of grey, open water being the darkest. The frame shows a lead that has frozen, partially closed, and opened again. Ice within the lead has rafted at many spots.

formations of a few percent on a time scale of a few days. Changes in the morphology of the ice pack are associated with these deformations. In divergence, new areas of open water are exposed. Convergence is accomplished by closing up any open water and, if necessary, by rearranging the thin ice to cover less area by building a rubble pile or pressure ridge. Shear is possible through slip along some cracks and the simultaneous creation of leads and pressure ridges. Each of these processes alters the thickness distribution.

The thermodynamic thickening of ice is described by a growth rate function f with dimensions of length per unit time. The magnitude of f is determined by the balance of the atmospheric and oceanic heat fluxes at the top and bottom of the ice, the thermal history of the ice, the thickness of the ice and

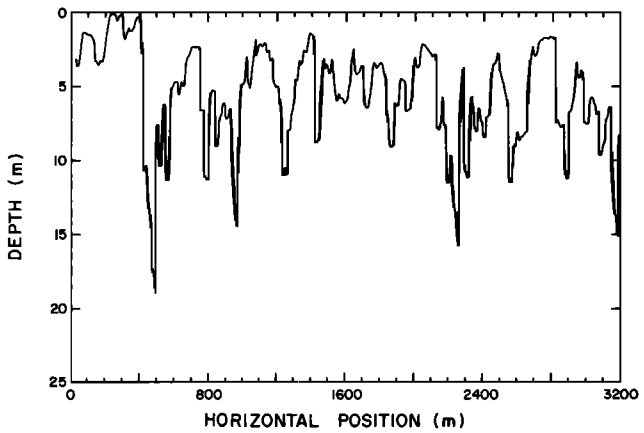

Fig. 2. A profile of the underside of arctic pack ice, after *Swithinbank* [1972]. The data were acquired from a submarine using upward-looking sonar at about 83°N, 06°E in March 1971.

overlying snow cover, and the distribution of liquid brine inclusions within the ice. Figure 5 illustrates the dependence of f on h in the central Arctic. During the winter, growth rates under 3-m perennial ice are nearly 2 orders of magnitude smaller than those in a refreezing lead. Summer growth rates are only weakly dependent on h, most of the mass change then occurring at the upper surface by melting. Seasonal changes in f are shown in Figure 6 for two different thicknesses of ice. While the thin ice responds almost immediately to changes in the atmospheric heat fluxes, thick ice behaves much more sluggishly. In fact, deep pressure ridge keels do not appear to be affected by seasonal changes at the upper surface and probably ablate throughout the year. While f does vary spatially, the limited data suggest that these variations are small over the perennially ice-covered portions of the Arctic Ocean. Although changes in the thickness distribution could alter the atmospheric and

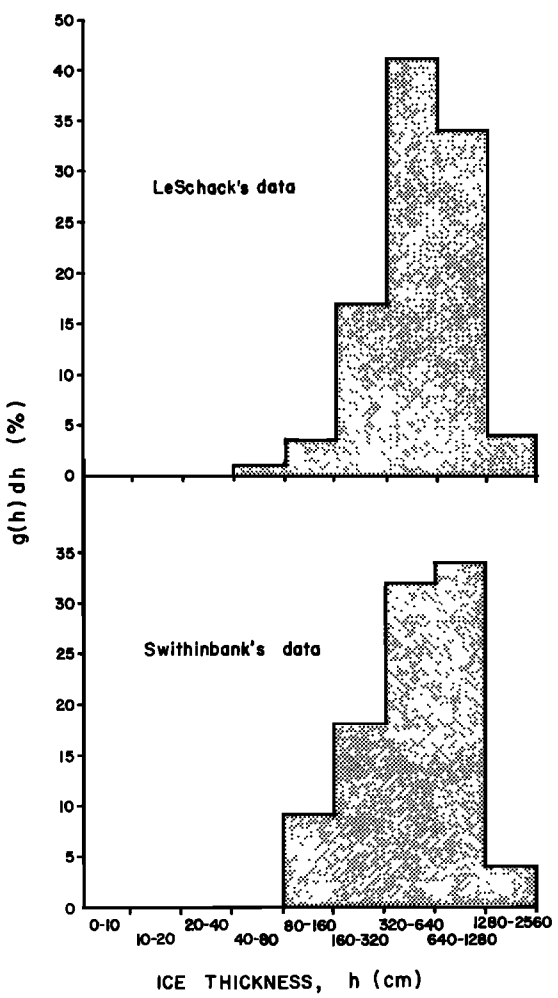

Fig. 3. Observed thickness distributions from *LeSchack et al.* [1971] and from an average of six profiles taken by *Swithinbank* [1972]. Both distributions describe winter conditions in the central Arctic.

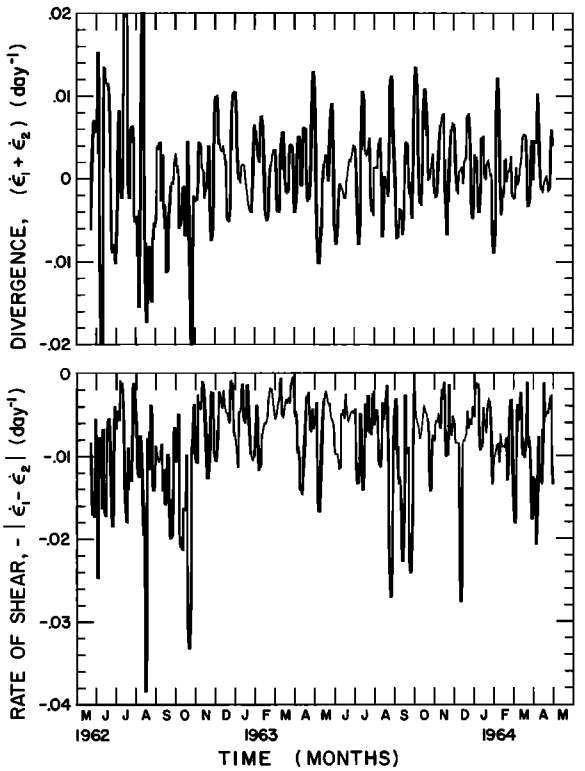

Fig. 4. The time series of the deformation rates calculated from position data of T-3, Arlis 2, and North Pole-10. The rate of divergence (above) is the sum of the principal rates of strain, $(\dot{\epsilon}_1+\dot{\epsilon}_2)$. The rate of shear is $-|\dot{\epsilon}_1-\dot{\epsilon}_2|$.

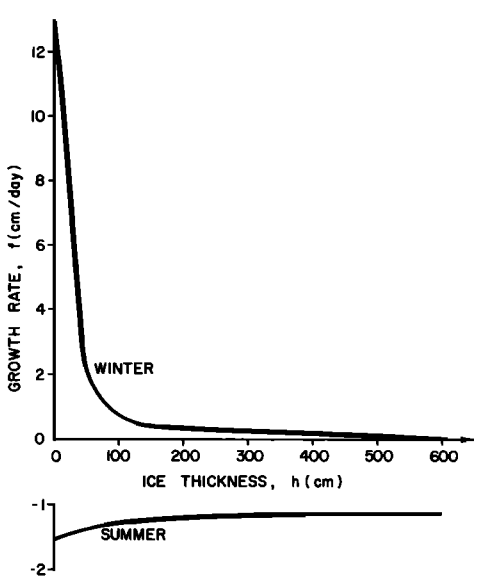

Fig. 5. Typical growth rates of sea ice in the central Arctic.

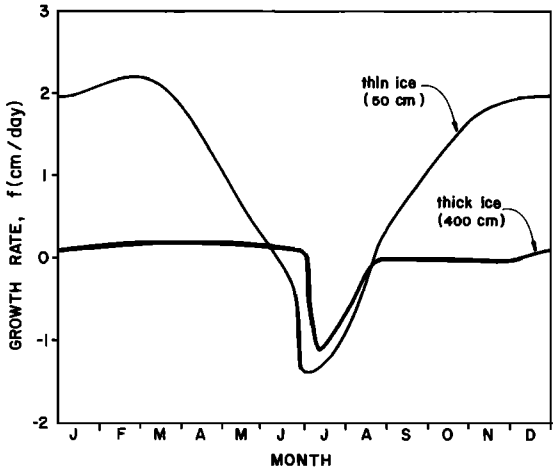

Fig. 6. Temporal variation of ice growth rates in the central Arctic.

oceanic boundary layers sufficiently to alter growth rates, we presently assume that growth rates can be determined outside the model and ignore this possible feedback.

Many of the bulk properties of the ice pack are completely determined by its thickness distribution, and other properties depend strongly on the thickness distribution and weakly on salinity, temperature, age, and snow cover. Consider, for example, the strength of the ice pack in compression. When substantial amounts of open water or very thin ice are present, the pack offers little resistance to compression, but if all the ice exceeds, say, a meter in thickness, the pack becomes extremely strong. A realistic constitutive relationship for the ice pack must therefore take account of the variable abundance of thin ice. This notion has been the primary motivation for this work.

The thickness distribution also influences the rate of heat input to the atmospheric and oceanic boundary layers. *Badgley* [1966] estimates that during much of the year, heat losses from open leads are 2 orders of magnitude greater than those over perennial ice. This means that if open water accounts for as little as 1% of the ice pack, then half of the heat lost by the ocean to the atmosphere must occur through the leads. The polar oceans also experience significant heating from shortwave radiation, which reaches the water primarily through leads and thin ice. Again, the abundance of thin ice and open water is the critical parameter.

Much of the gravitational and buoyant potential energy of the ice pack is tied up in the thick pressure ridges. We assume the work required to deform the ice pack goes into the potential energy of the ridges and neglect the energy dissipated by friction. The ridges also give ice its characteristic topography and must be considered in estimates of the wind and water drag on the ice.

THEORY

The definition of $g(h)$, stated in (1), applies to a region **R**. It will be useful to extend the definition to apply at any particular Eulerian point **x**. Letting the region collapse to a point is unacceptable since each point has only a single thickness and the concept of a distribution, in that case, would not be helpful. Instead, we define for each point **x** a region **R**(**x**) containing **x** and with some characteristic length scale, for example, **R**(**x**) might be a circular neighborhood of radius 100 km centered at **x**. Under such a definition, both A and g in (1) become functions of **x**. The length scale should be large enough for **R**(**x**) to contain a representative sample of ice types, so that, under small changes in **x**, g will vary smoothly, but small enough to resolve the regional variations in g. Ignoring the structure within **R**, we assume that every subregion of **R**(**x**) has nearly the same thickness distribution as **R**(**x**) does itself. This continuum hypothesis, as false here as it is in its application to other more familiar materials, is invoked for the same reason: to justify the application of continuous mathematics to a highly discrete physical system.

Our formulation could have included the density of the ice and defined a distribution of mass per unit area. At this writing, however, thickness seems to be more useful for describing the thermodynamic and the mechanical behavior of the ice. If at some time it becomes important to include density effects, such as when the presence of voids reduces the effective density of ridges, this can be done within the framework of the present ice thickness distribution theory. For the present we take the density of the ice to be a constant.

The ice thickness h can assume values from zero, where it represents open water, to some upper bound h_{max}. Outside of these limits, $g(h)$ always vanishes. Integrating (1) between those limits gives

$$\int_0^{h_{max}} g(h)\, dh = 1 \qquad (2)$$

When a finite area of ice has a uniform thickness h_1, then $\lim_{h_2 \downarrow h_1} A(h_1, h_2)$ is finite and $g(h)$ must be a delta function at h_1. Such a situation occurs at $h = 0$ toward the end of each summer when several percent of the ocean surface is ice free. With the onset of freezing in the fall the delta function begins to move to the right in h space with a speed f, as the once ice-free area now assumes a thickening integument of young ice.

At times it will be more natural to refer to the cumulative thickness distribution $G(h, t, \mathbf{x})$, $(=\int_0^h g(h', t, \mathbf{x})\, dh')$ which is the fractional area of ice thinner than h. We can interpret $g(h, t, \mathbf{x})$ and $G(h, t, \mathbf{x})$ as a probability density function and its cumulative probability function. We should then think of h as the random variable and t and **x** as parameters indicating that the distribution may vary in time and space. Both points of view are valid and useful; for the most part, however, we will confine ourselves to the area interpretation of these functions.

BASIC EQUATION

The thickness distribution is subject to changes brought about by advection, by mechanical processes, and by thermodynamic growth or melt.

That the ice moves about on the surface of the ocean implies that g will change as areas of ice of different thicknesses are advected into the region **R**. Conceptually, we replace the highly detailed velocity field of the ice pack with a velocity **v** which is smoothed sufficiently to be nearly linear over **R**. At a point **x'** on the boundary of **R** an area of ice is carried into or out of **R**, which, invoking the continuum hypothesis claimed earlier, has the thickness distribution $g(h, \mathbf{x}', t)$. We may think then of a flux of the thickness distribution itself, $\mathbf{v}g$, and equate the time rate of change in g to the divergence of this flux $-\nabla\cdot(\mathbf{v}g)$. The mechanical ridging and opening processes, by rearranging ice already in **R**, can be viewed as sources and sinks of the area of ice of each thickness. The rate of change of g by these effects is parameterized in the redistribution function ψ which we will discuss below.

The change caused by ice growing or melting is more easily written in terms of G, the cumulative distribution. Because ice changes its thickness thermodynamically at a rate f, all of the

ice which is thinner than h at time t will be thinner than $h + f\,dt$ at time $t + dt$. Thus

$$G(h, t) = G(h + f\,dt, t + dt)$$

$$= G(h, t + dt) + f\,dt\frac{\partial G}{\partial h} + \text{terms in } dt^2$$

which can be rearranged to show that $\partial G/\partial t = -f\,\partial G/\partial h$. Differentiating with respect to h gives $\partial g/\partial t = -\partial/\partial h\,(fg)$.

Combining these three processes, we have the governing equation for the thickness distribution

$$\frac{\partial g}{\partial t} = -\nabla\cdot(\mathbf{v}g) - \frac{\partial}{\partial h}(fg) + \psi \tag{3}$$

The growth rate f is taken to depend on h, $\mathbf{x}$, and t, whereas the velocity is a function of $\mathbf{x}$ and t only. Notice the analogous roles played by the velocity $\mathbf{v}$ and the growth rate f.

The redistribution function. Here, and in the following two sections, we will describe how the redistribution function ψ depends on h, on the strain rate defined in terms of the smoothed velocity field, and, as a functional, on the thickness distribution g.

ψ must satisfy two strong constraints. The first of these is the conservation of the total area of ice in $\mathbf{R}$. During an episode of deformation there will be a flux of ice area out of $\mathbf{R}$ at a rate div $\mathbf{v}$, but since the total area of $\mathbf{R}$ is fixed, ψ must compensate for any loss or gain of area. By integrating each term in (3) over all thicknesses and recalling (2), we see that

$$\int_0^{h_{max}} \psi\,dh = \text{div } \mathbf{v} \tag{4}$$

The integral of the third term in (3) represents the change of total area by thermodynamics which must be zero.

The second constraint arises from our making the simplest possible assumption about the redistribution process, namely, that ridging, by itself, does not change the volume of ice per unit area, requiring

$$\int_0^{h_{max}} h\psi\,dh = 0$$

Of course, the volume can be changed, but this is accomplished by the second term in equation (3).

To deduce the form of ψ, we consider separately the cases of pure divergence and pure convergence and later combine them to account for shearing.

When the ice is diverging, we assume that open water is produced to fill in the area exported from $\mathbf{R}$. This is accomplished by a delta function at $h = 0$:

$$\psi = \delta(h)\,\text{div } \mathbf{v} \tag{5}$$

in pure divergence. Although this assumption may seem obvious, it does rule out, for example, the possibility that the existing ice merely stretches uniformly.

The ridging mode. In the more difficult case of pure convergence (div $\mathbf{v} < 0$) the term $-g$ div $\mathbf{v}$ causes a flux of ice into $\mathbf{R}$, and ψ must make room for this new ice by rearranging the ice already in $\mathbf{R}$ to occupy less area. This is accomplished by taking thin ice from a range of ice thicknesses, including but not limited to the very thinnest ice, and building pressure ridges so that the area covered by thin ice is decreased, while the area covered by thick ice is increased. Thus ψ is negative for some range of thin ice and positive for a range of thick ice. We write ψ, then, as

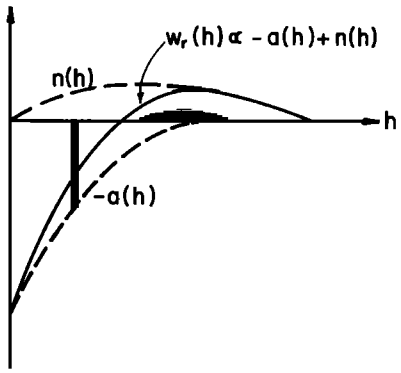

Fig. 7. The ridging mode $w_r(h)$ as the sum of two distributions: $-a(h)$, the ice being broken up to provide the material in ridges, and $n(h)$, the thicker ridged ice.

$$\psi = w_r(h, g)\,\text{div } \mathbf{v} \tag{6}$$

in pure convergence. In this expression it is assumed that the manner in which ψ depends on h and on the thickness distribution is the same regardless of how fast the convergence is occurring. We call w_r the ridging mode, and, of course, it depends on h in the same way as ψ: negative for thin ice and positive for thick ice. Furthermore, the area and volume conservation constraints on ψ translate into equivalent constraints on $w_r(h)$

$$\int_0^{h_{max}} w_r(h)\,dh = -1$$

and

$$\int_0^{h_{max}} hw_r(h)\,dh = 0$$

The actual form of $w_r(h)$ depends on g, as a functional, in a way we must hypothesize. We do so in several steps by (1) specifying the thickness distribution $a(h)$ of the ice participating in the ridging; (2) specifying the rule by which the participating ice of some thickness is transformed into thicker ridged ice, in a way that conserves volume; (3) calculating the distribution $n(h)$ of the newly ridged ice; and (4) forming $w_r(h)$ from the sum of $-a(h)$ and $n(h)$, normalized to guarantee that $\int_0^\infty w_r\,dh = -1$.

The ridging mode can be viewed, then, as the sum of a number of events in which some area of thin ice represented by the column on the left in Figure 7 is transformed by the rule in step 2 into areas in a range of thicker ice represented by the shaded area in the figure. The sum of all the columns forms $-a(h)$; the set of solid areas adds up to $n(h)$.

In the remainder of this section we relate $a(h)$ and $n(h)$ to $g(h)$ and present an example. The reader who prefers to follow the primary line of argument might profitably presume $w_r(h)$ to be given and skip to the next section.

The development of $a(h)$ and $n(h)$ is most clearly rendered by distinguishing two thicknesses of ice: h_1, the thickness of ice participating in the ridging, and h_2, the thickness of the resulting deformed ice. The distribution a is defined such that $a(h_1)\,dh_1$ is the fractional area in the thickness range $(h_1, h_1 + dh_1)$ of all the ice participating instantaneously in ridging. Clearly, a is related to g since it would make no sense to have ice of some particular thickness participate in ridging if g told us that no ice of that thickness existed. It is not simply the thinnest ice, say, h_0, that ridges ($a(h_1) = \delta(h_1 - h_0)$) because stress

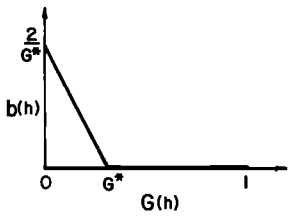

Fig. 8. The weighting function $b(h)$ given by (7).

concentrations associated with the irregular geometries of floes and leads cause thicker ice to fail. Neither do we think that ice of all thicknesses ridges ($a(h_1) = g(h_1)$). We hypothesize that for real (chaotic) arrangements of ice, $a(h_1)$ lies in between these two extremes. We suspect that ice of any thickness may ridge but that the thinner a piece of ice is, the weaker it is and the more likely it is to become involved in ridging.

To formalize this notion, we postulate that $a(h)$ can be obtained by multiplying $g(h)$ by a weighting function which accentuates the thin end of the thickness distribution. For a given cumulative thickness distribution G the range of ice thicknesses most likely to participate in ridging will be associated with the lowest values of G. A weighting function $b(h)$ which reflects this must be monotonic decreasing in G. One such function, which we have used here, is

$$b(h) = \frac{2}{G^*}\left[1 - \frac{G(h)}{G^*}\right] \qquad 0 \le G(h) \le G^*$$
$$b(h) = 0 \qquad G(h) > G^* \tag{7}$$

where G^* is taken as some arbitrary fraction below which all ridging occurs (see Figure 8). Thus

$$a(h) = b(h)g(h) \tag{8}$$

One result of this formulation is that if open water covers as large a fraction of the area as G^*, the ridging mode will only close up open water until such time as the fraction of open water falls below G^* and ridging can resume. In the summer when floes are fairly round and the pack looks granular, a plausible value for G^* would be 0.15. As a point of comparison, the void surrounding closely packed circles on a plane is $1 - \pi/(2(3)^{1/2})$, or about 0.09, and the void surrounding a circle inscribed in a square is $1 - \pi/4$, or about 0.21. The factor $2/G^*$ in (7) is chosen to normalize $a(h)$ so that its integral over all thicknesses is unity. The thickest ice ridging is of thickness h^* where $G(h^*) = G^*$. Ice thicker than h^* affects neither $a(h)$ nor $w_r(h)$.

In general, if we take a unit area of ice of some particular thickness h_1 and make pressure ridges out of it, we would get ridged ice with a distribution of thicknesses $\gamma(h_1, h_2)$; that is, $\gamma(h_1, h_2)\,dh_2$ is the area of ice put into the thickness interval $(h_2, h_2 + dh_2)$ when a unit area of ice of thickness h_1 is used up. Referring to Figure 7, $\gamma(h_1, h_2)$ gives the height of the shaded area at all values of $h = h_2$ for a column of unit height at $h = h_1$.

We assume that γ, called the redistribution process, conserves volume for each thickness of ice being ridged:

$$\int_0^{h_{max}} h_2\gamma(h_1, h_2)\,dh_2 = h_1$$

The distribution of the newly ridged ice is found easily in terms of γ and a:

$$n(h_2) = \int_0^{h_{max}} \gamma(h_1, h_2)a(h_1)\,dh_1$$

Note that a unit area of ice being ridged is converted into an area

$$\int_0^{h_{max}} n(h_2)\,dh_2$$

of ridged ice which will always be less than one. At any given h, $a(h)$ represents a decrease in $g(h)$, and $n(h)$ represents an increase. Thus w_r is defined by step 4 to be

$$w_r(h) = \frac{-a(h) + n(h)}{-\int_0^{h_{max}} [-a(h) + n(h)]\,dh}$$

With very little data from which a realistic $\gamma(h_1, h_2)$ could be constructed we settle here for the assumption that all ridged ice is k times its original thickness, making

$$\gamma = \frac{1}{k}\delta(h_2 - kh_1) \tag{9}$$

Then we have

$$n(h_2) = \frac{1}{k}\int_0^{h_{max}} \delta(h_2 - kh_1)a(h_1)\,dh_1 = \frac{1}{k^2}\,a\left(\frac{h_2}{k}\right) \tag{10}$$

and

$$w_r(h) = \frac{-a(h) + (1/k^2)a(h/k)}{1 - (1/k)} \tag{11}$$

We will use the value $k = 5$, this being a reasonable estimate from the ridging study of *Parmerter and Coon* [1972].

The following simple example will illustrate how $w_r(h)$ is formed from $g(h)$. We use expressions (7) and (9). Suppose that $g(h)$ equals g_1, a constant, for at least the thin ice ($h \le h^*$), as in Figure 9. Then, G equals g_1h for $h \le h^*$, and h^* has the value G^*/g_1. The distributions $a(h)$ and $n(h)$ become

$$a(h) = \frac{2}{h^*}\left(1 - \frac{h}{h^*}\right) \qquad h \le h^*$$
$$a(h) = 0 \qquad h > h^*$$

and

$$n(h) = \frac{2}{k^2h^*}\left(1 - \frac{h}{kh^*}\right) \qquad h \le kh^*$$
$$n(h) = 0 \qquad h > kh^*$$

from (8) and (10). Then $w_r(h)$ is formed from the scaled sum $(-a + n)/[1 - (1/k)]$ as shown in (11) and in Figure 9. For further examples see *Thorndike and Maykut* [1973] and *Coon et al.* [1974].

Redistribution of ice under an arbitrary strain rate. The redistributor ψ is a function of the strain rate tensor. We assume that the ice has no directional properties, so that ψ depends only on two invariants of the strain rate tensor: $\dot{\epsilon}_I$, the sum of the principal values, being the divergence of velocity, and $\dot{\epsilon}_{II}$, the difference between the principal values, being related to the shearing.

At this time we can make only qualitative and intuitive arguments for how ψ depends on the strain rate invariants (except when $\dot{\epsilon}_I > 0$ and $\dot{\epsilon}_{II} = 0$, about which we are more confident). That ψ is active, even during pure shear when $\dot{\epsilon}_I = \text{div } \mathbf{v} = 0$, is a consequence of the following reasoning. The pack ice is par-

titioned into discrete quasi-rigid floes by a dense network of irregular jagged cracks. When shearing occurs, the displacement vector at any point along a crack may have any orientation with respect to the crack, depending on which way the crack trends locally. In Figure 10 we imagine different segments of cracks opening, closing, and shearing, all in response to the same applied strain rate. The ice thickness distribution is not affected by components of the displacement parallel to the crack, but the components normal to the crack will cause local deformation and redistribution similar to the ridging and opening cases treated above. The deformation indicated in Figure 10 is pure shear, and still there are some cracks opening and some closing.

The conclusion is that shearing can alter the thickness distribution but that it does so by exercising the same ridging and opening modes involved in pure convergence and pure divergence. In general, then, the redistributor is the sum of two modes:

$$\psi = (\dot{\epsilon}_I^2 + \dot{\epsilon}_{II}^2)^{1/2}\{\alpha_0(\theta)w_0 + \alpha_r(\theta)w_r\} \tag{12}$$

where $w_0 = \delta(h)$ and w_r are the opening and ridging modes and depend only on h and g. The coefficients α_0 and α_r depend only on θ, which is defined as $\tan^{-1}(\dot{\epsilon}_{II}/\dot{\epsilon}_I)$ and is a measure of the relative rates of shearing and divergence. In effect, (8) represents the redistributor in terms of a new pair of strain rate invariants $(\dot{\epsilon}_I^2 + \dot{\epsilon}_{II}^2)^{1/2}$ and θ. The magnitude of ψ is determined by $(\dot{\epsilon}_I^2 + \dot{\epsilon}_{II}^2)^{1/2}$, while the amount of opening and ridging are determined by θ. The relative amounts of opening and ridging, and thus the manner in which ψ depends on h, are assumed to be affected by θ but not by the rate of deformation.

To reproduce the case of pure divergence (5), $\alpha_0(\theta = 0)$ must equal 1, and $\alpha_r(\theta = 0)$ must be zero. Similarly, $\alpha_0(\pi) = 0$ and $\alpha_r(\pi) = 1$ ensure that (6) is retained in pure convergence. Both α_0 and α_r are even functions of θ and of $\pi - \theta$ and need be defined only in the range $[0, \pi]$. Assuming that ridges freeze as soon as they are formed so that there is no 'unridging,' we require that $\alpha_r \geq 0$ for all θ. We also require that the coefficient of the opening mode never be negative ($\alpha_0 \geq 0$); when convergence can occur simply by closing open water ($h^* = 0$), the ridging mode will accomplish this. Area conservation provides a simple relation between α_0 and α_r. Inserting (12) into (4) and recalling that $\int_0^{h_{max}} w_0\, dh = 1$ and $\int_0^{h_{max}} w_r\, dh = -1$, we obtain

$$\alpha_0(\theta) - \alpha_r(\theta) = \cos\theta$$

The forms assumed here, $\alpha_r = \frac{1}{2}(1 - \cos\theta)$ and $\alpha_0 = \frac{1}{2}(1 + \cos\theta)$, vary smoothly between zero and unity.

The mean thickness and yield strength of the ice pack. If a property ϕ is known to depend on ice thickness h, then the bulk property is defined as

$$\bar{\phi} = \int_0^{h_{max}} \phi(h)g(h)\, dh$$

The mean thickness $\bar{h}$ must satisfy

$$\frac{d\bar{h}}{dt} \equiv \frac{\partial \bar{h}}{\partial t} + \mathbf{v}\cdot\mathrm{grad}\,\bar{h} = \bar{f} - \bar{h}\,\mathrm{div}\,\mathbf{v} \tag{13}$$

which is obtained by operating on (3) with $\int_0^{h_{max}} h \cdot (\ )\, dh$. The term $-\int_0^{h_{max}} h\, \partial/\partial h\, (fg)\, dh$ has been integrated by parts.

The concept of a critical compressive strength p^* below which the ice pack is rigid and at which it fails can be used to develop a full model of the mechanical behavior of the pack [*Coon et al.*, 1974]. When the pack fails in compression, work is done by displacing the ice against the resistance p^*. At the same time the thickness distribution changes under the influence of ψ. Assuming the ice is in isostatic balance everywhere, the ice has an amount of gravitational and buoyant potential energy proportional to the square of its thickness. Thus as the thickness distribution changes, the total amount of potential energy may also change as, under ψ, thin ice of low potential energy is converted into thick ice of greater potential energy. The frictional losses, which accompany this process but are ignored here, are of the same order as the potential energy production [*Rothrock*, 1975]. By insisting that the rate of work per unit area by a compressive deformation div v (s^{-1}) against a strength p^* (dyn cm^{-1}) is equal to the rate of potential energy production per unit area due to the redistribution process, we can relate p^* to w_r and thereby to g:

$$-p^*\,\mathrm{div}\,\mathbf{v} = c\int_0^\infty h^2\psi(h)\, dh = |\mathrm{div}\,\mathbf{v}|c\int_0^\infty h^2 w_r(h)\, dh \tag{14}$$

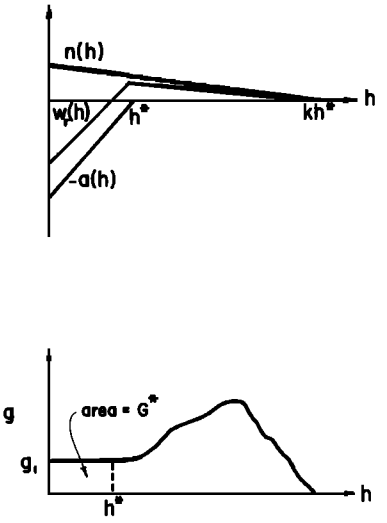

Fig. 9. The distributions $a(h)$, $n(h)$, and $w_r(h)$ obtained from (4), (5), (6), and (7) for the illustrated thickness distribution.

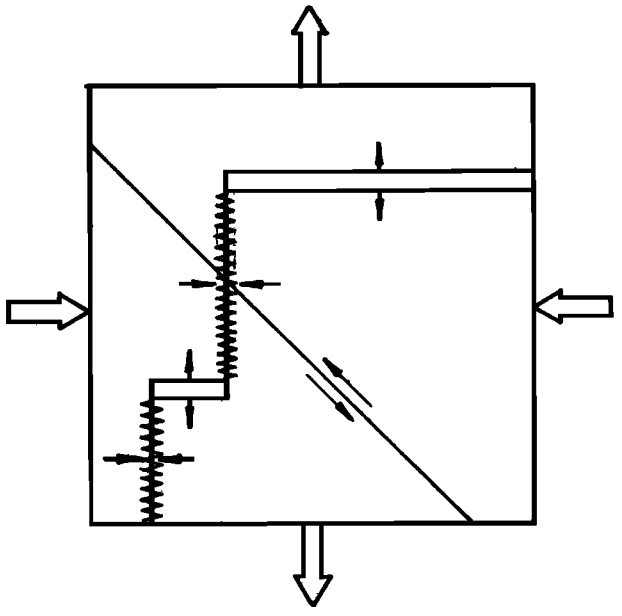

Fig. 10. Schematic diagram illustrating the formation of leads and pressure ridges during pure shearing deformation.

TABLE 1. Growth Rates of Sea Ice in Centimeters per Day

Date	0 cm	50 cm	100 cm	150 cm	200 cm	250 cm	300 cm	350 cm	400 cm	450 cm
Jan. 1	12.09	1.95	0.46	0.37	0.31	0.27	0.21	0.14	0.09	0.03
Jan. 11	12.15	1.97	0.51	0.37	0.32	0.27	0.21	0.17	0.11	0.06
Jan. 21	12.29	2.00	0.57	0.37	0.32	0.27	0.22	0.18	0.13	0.07
Feb. 1	12.49	2.07	0.63	0.37	0.32	0.27	0.23	0.19	0.15	0.09
Feb. 11	12.67	2.11	0.68	0.37	0.32	0.28	0.25	0.20	0.16	0.10
Feb. 21	12.82	2.16	0.73	0.39	0.34	0.29	0.25	0.20	0.17	0.11
March 1	12.90	2.18	0.77	0.40	0.34	0.29	0.25	0.21	0.17	0.12
March 11	12.71	2.13	0.80	0.39	0.34	0.29	0.26	0.23	0.18	0.13
March 21	12.38	2.03	0.81	0.38	0.34	0.29	0.26	0.23	0.19	0.13
April 1	11.71	1.86	0.41	0.36	0.32	0.29	0.25	0.23	0.20	0.14
April 11	10.82	1.63	0.36	0.32	0.29	0.27	0.25	0.23	0.20	0.14
April 21	9.69	1.36	0.34	0.28	0.26	0.25	0.23	0.22	0.19	0.14
May 1	8.18	1.03	0.27	0.22	0.22	0.22	0.21	0.21	0.18	0.14
May 11	6.88	0.78	0.21	0.17	0.18	0.18	0.19	0.18	0.17	0.13
May 21	5.16	0.50	0.13	0.12	0.14	0.15	0.15	0.16	0.16	0.12
June 1	3.10	0.24	0.05	0.07	0.09	0.11	0.12	0.14	0.14	0.12
June 11	0.00	0.00	−0.00	0.03	0.05	0.08	0.09	0.11	0.12	0.10
June 21	−0.65	−0.20	−0.08	−0.01	0.02	0.05	0.07	0.08	0.10	0.08
July 1	−1.60	−1.40	−1.32	−1.28	−1.25	−1.21	−1.16	−0.40	0.07	0.07
July 11	−1.55	−1.35	−1.25	−1.22	−1.19	−1.17	−1.14	−1.12	−1.11	−1.10
July 21	−1.40	−1.20	−1.07	−1.04	−1.01	−0.99	−0.97	−0.94	−0.93	−0.93
Aug. 1	−1.00	−0.90	−0.84	−0.80	−0.77	−0.75	−0.72	−0.71	−0.69	−0.70
Aug. 11	−0.65	−0.55	−0.52	−0.49	−0.46	−0.43	−0.42	−0.40	−0.39	−0.38
Aug. 21	0.13	0.01	−0.17	−0.14	−0.10	−0.06	−0.04	−0.02	−0.00	−0.00
Sept. 1	4.08	0.36	−0.16	−0.14	−0.10	−0.07	−0.05	−0.03	−0.01	−0.01
Sept. 11	5.50	0.56	−0.12	−0.13	−0.10	−0.07	−0.06	−0.04	−0.02	−0.02
Sept. 21	6.81	0.77	0.06	−0.12	−0.10	−0.08	−0.06	−0.05	−0.03	−0.03
Oct. 1	8.05	1.01	0.25	−0.03	−0.09	−0.08	−0.07	−0.05	−0.03	−0.03
Oct. 11	9.01	1.21	0.34	0.10	−0.05	−0.07	−0.06	−0.05	−0.04	−0.04
Oct. 21	9.99	1.43	0.40	0.20	0.04	−0.04	−0.06	−0.05	−0.05	−0.04
Nov. 1	10.97	1.66	0.48	0.26	0.12	0.02	−0.03	−0.04	−0.04	−0.04
Nov. 11	11.55	1.81	0.55	0.30	0.19	0.08	0.00	−0.02	−0.03	−0.03
Nov. 21	11.95	1.92	0.62	0.34	0.25	0.14	0.05	0.00	−0.02	−0.02
Dec. 1	12.06	1.95	0.44	0.35	0.28	0.20	0.11	0.04	0.00	−0.01
Dec. 11	12.04	1.94	0.44	0.37	0.30	0.23	0.15	0.08	0.03	−0.00
Dec. 21	12.04	1.94	0.44	0.38	0.31	0.25	0.19	0.12	0.06	0.01

(in pure compression). The constant c depends on the acceleration of gravity $\hat{g}$ and on the densities of ice and water, ρ_{ice} and ρ_{water}, in the combination

$$c = \tfrac{1}{2}\hat{g}\rho_{ice}(\rho_{water} - \rho_{ice})/\rho_{water}$$

Equation (14), then, provides us with a measure of the strength of the pack in terms of the thin end of the thickness distribution.

Notice that the strength of the pack is defined by (14) in terms of changes in potential energy and not in terms of the mechanical properties of sea ice as they might be measured in a laboratory test. While the important properties of sea ice itself may be its elastic moduli or its plastic strength, we believe the important properties of the ice pack are its highly and randomly fractured nature, its characteristic modes of deformation (the formation of ridges and leads, as modeled in ψ), and, above all, its thickness distribution.

BEHAVIOR OF THE MODEL

Input data. The theory for the thickness distribution equation and the redistribution function was constructed by thinking of isolated processes driven by simple deformational events. Here we drive the equation simultaneously with our best estimate of growth rates and a 2-year history of observed straining to see how the model behaves under real forcing. A shorter but similar calculation, as well as a series of calculations for artificial cases, i.e., no motion, isotropic motion, uniaxial motion, and pure shear, were described by *Coon et al.* [1974].

The thermodynamic growth rates were derived from climatological heat fluxes and air temperatures using empirical results for thin ice [*Anderson,* 1961], theoretical calculations for ice of 1–4 m [*Maykut and Untersteiner,* 1971], and fragmentary observation, theory, and intuition for thick ice. The array of values from which interpolations were made to any thickness and time is reproduced in Table 1.

The deformations used here are taken from the observed motion of three drifting stations, T-3, Arlis 2, and NP-10, which were manned by U.S. and Russian scientists from 1962 to 1964 (Figure 11). The reported positions of these stations were edited and smoothed and then reduced to strain rate invariants (Figure 4) which were then used to derive the thickness distribution calculations. In the standard case the initial condition for the calculations, shown in Figure 12*a*, was taken from one of several distributions derived from the underice profiles of *Swithinbank* [1972].

The numerical procedure. We have solved the basic equation (3) in the form

$$\frac{dG}{dt} + f\frac{\partial G}{\partial h} = \Psi - G \operatorname{div} \mathbf{v}$$

where $\partial/\partial t + \mathbf{v}\cdot\operatorname{grad}$ has been replaced by the Lagrangian operator d/dt to apply to the region defined by the three drifting stations. Ψ is defined as $\int_0^h \psi(h')\,dh'$. This partial

as a Function of Thickness (0–1000 cm) and Time of Year

500 cm	550 cm	600 cm	650 cm	700 cm	750 cm	800 cm	850 cm	900 cm	950 cm	1000 cm
0.00	−0.02	−0.03	−0.04	−0.05	−0.05	−0.06	−0.06	−0.06	−0.06	−0.06
0.02	−0.01	−0.03	−0.04	−0.04	−0.05	−0.06	−0.06	−0.06	−0.06	−0.06
0.03	0.00	−0.02	−0.04	−0.04	−0.05	−0.06	−0.06	−0.06	−0.06	−0.06
0.05	0.01	−0.02	−0.03	−0.04	−0.05	−0.06	−0.06	−0.06	−0.06	−0.06
0.05	0.01	−0.01	−0.03	−0.04	−0.05	−0.06	−0.06	−0.06	−0.06	−0.06
0.06	0.02	−0.01	−0.02	−0.04	−0.05	−0.06	−0.06	−0.06	−0.06	−0.06
0.07	0.03	−0.00	−0.02	−0.04	−0.05	−0.06	−0.06	−0.06	−0.06	−0.06
0.08	0.04	0.00	−0.02	−0.04	−0.05	−0.06	−0.06	−0.06	−0.06	−0.06
0.08	0.04	0.01	−0.02	−0.03	−0.05	−0.06	−0.06	−0.06	−0.06	−0.06
0.09	0.05	0.01	−0.01	−0.03	−0.05	−0.06	−0.06	−0.06	−0.06	−0.06
0.09	0.05	0.02	−0.01	−0.03	−0.05	−0.06	−0.06	−0.06	−0.06	−0.06
0.10	0.06	0.02	−0.01	−0.03	−0.05	−0.06	−0.06	−0.06	−0.06	−0.06
0.10	0.06	0.03	−0.00	−0.03	−0.04	−0.06	−0.06	−0.06	−0.06	−0.06
0.09	0.06	0.03	−0.00	−0.03	−0.04	−0.06	−0.06	−0.06	−0.06	−0.06
0.09	0.06	0.03	−0.00	−0.02	−0.04	−0.06	−0.06	−0.06	−0.06	−0.06
0.08	0.05	0.02	−0.00	−0.02	−0.04	−0.06	−0.06	−0.06	−0.06	−0.06
0.07	0.05	0.02	−0.00	−0.02	−0.04	−0.06	−0.06	−0.06	−0.06	−0.06
0.06	0.04	0.02	−0.00	−0.03	−0.04	−0.06	−0.06	−0.06	−0.06	−0.06
0.05	0.03	0.02	−0.00	−0.03	−0.04	−0.06	−0.06	−0.06	−0.06	−0.06
−1.11	−1.13	−1.15	−1.17	−1.18	−1.20	−1.20	−1.20	−1.20	−1.20	−1.20
−0.93	−0.94	−0.96	−0.97	−0.99	−1.00	−1.00	−1.00	−1.00	−1.00	−1.00
−0.70	−0.71	−0.71	−0.73	−0.74	−0.75	−0.75	−0.75	−0.75	−0.75	−0.75
−0.38	−0.39	−0.39	−0.41	−0.42	−0.43	−0.43	−0.43	−0.43	−0.43	−0.43
0.00	−0.01	−0.02	−0.02	−0.04	−0.05	−0.06	−0.06	−0.06	−0.06	−0.06
−0.01	−0.01	−0.02	−0.02	−0.04	−0.05	−0.06	−0.06	−0.06	−0.06	−0.06
−0.02	−0.01	−0.02	−0.03	−0.04	−0.05	−0.06	−0.06	−0.06	−0.06	−0.06
−0.02	−0.02	−0.02	−0.03	−0.04	−0.05	−0.06	−0.06	−0.06	−0.06	−0.06
−0.02	−0.02	−0.03	−0.03	−0.04	−0.05	−0.06	−0.06	−0.06	−0.06	−0.06
−0.03	−0.03	−0.03	−0.04	−0.04	−0.05	−0.06	−0.06	−0.06	−0.06	−0.06
−0.03	−0.03	−0.03	−0.04	−0.04	−0.05	−0.06	−0.06	−0.06	−0.06	−0.06
−0.03	−0.03	−0.03	−0.04	−0.04	−0.05	−0.06	−0.06	−0.06	−0.06	−0.06
−0.03	−0.03	−0.03	−0.04	−0.04	−0.05	−0.06	−0.06	−0.06	−0.06	−0.06
−0.03	−0.03	−0.03	−0.04	−0.05	−0.05	−0.06	−0.06	−0.06	−0.06	−0.06
−0.03	−0.03	−0.03	−0.04	−0.05	−0.05	−0.06	−0.06	−0.06	−0.06	−0.06
−0.00	−0.02	−0.03	−0.04	−0.05	−0.05	−0.06	−0.06	−0.06	−0.06	−0.06
−0.01	−0.02	−0.03	−0.04	−0.05	−0.05	−0.06	−0.06	−0.06	−0.06	−0.06

differential equation is equivalent to the pair of ordinary differential equations

$$dh/dt = f(h, t) \tag{15}$$

$$DG/Dt = \Psi - G \operatorname{div} \mathbf{v} \tag{16}$$

The first equation defines a set of characteristics in (h, t) space, and the second describes how G changes following those characteristics. In addition to the initial condition $G(h, t = 0)$ we must specify boundary conditions at $h = 0$ and $h = h_{max}$. These are that $G(0, t) = 0$ and $G(h_{max}, t) = 1$ except when $f < 0$ at $h = 0$ or $f > 0$ at $h = h_{max}$, at which times it would over-determine the problem to specify G.

The numerical procedure has four steps:

1. Choose an ordered partition $\{h_i\}$, $i = 1, N$ with $h_1 = 0$, $h_N = h_{max}$. The partition can be arbitrary with small intervals ($h_i - h_{i-1} \simeq 0$) at points where $\partial G/\partial h$ is large.
2. Assume $G_i = G(h_i, t)$, $i = 1, N$ are known at some time t. For a time step Δt, integrate (15) and (16) to obtain $\hat{h}_i$ and $\hat{G}_i$ using the standard fourth-order Runge-Kutta method [*Hildebrand*, 1962]. In this integration, Ψ is evaluated at any point h using the tabular function $\{h_i, G_i\}$, $i = 1, N$.
3. If increased resolution is desired, as it probably will be for thin ice when $f(0, t) > 0$, additional characteristics can be added beginning at $h = 0$ and at times between t and $t + \Delta t$ and integrated forward to time $t + \Delta t$. This will produce an additional set of points $\{\tilde{h}_i, \tilde{G}_i\}$, $i = 1, M$.
4. Using the new points $\{\hat{h}_i, \hat{G}_i\}$, $i = 1, N$, and $\{\tilde{h}_i, \tilde{G}_i\}$, $i =$

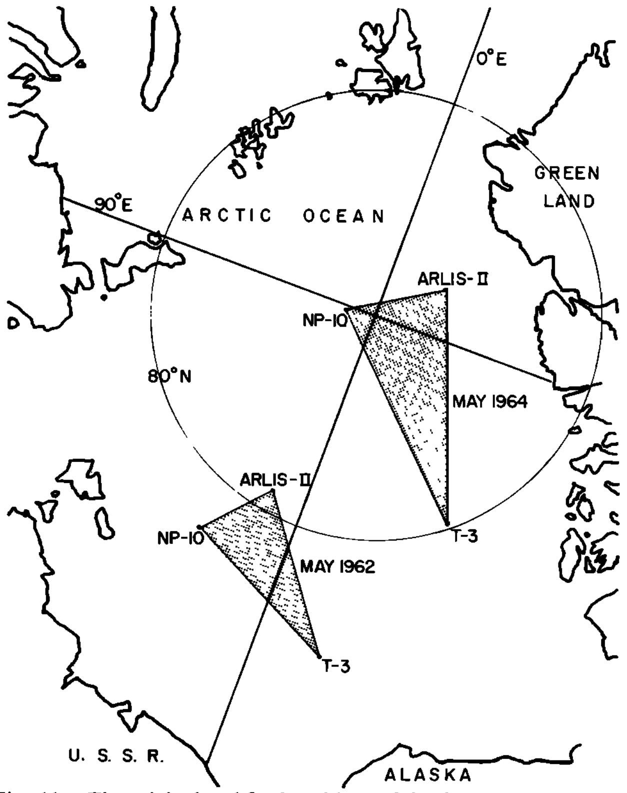

Fig. 11. The original and final positions of the three drifting stations used to define a 2-year strain history.

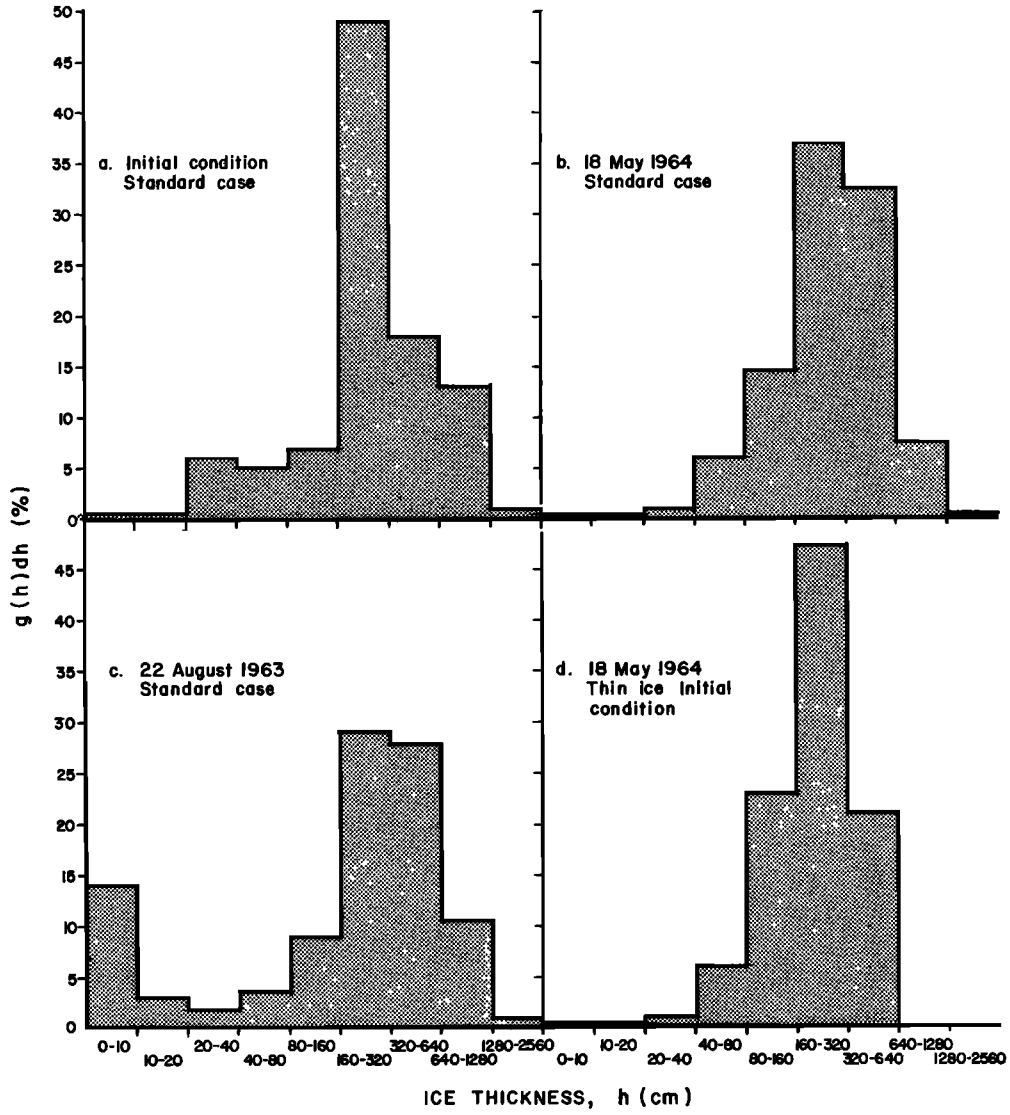

Fig. 12. The thickness distribution (*a*) assumed as an initial condition, (*b*) after 2 years, (*c*) in late August 1963, and (*d*) after 2 years, beginning with no ice thicker than 20 cm.

1, M, interpolate to find $G_i = G(h_i, t + \Delta t)$ at the original partition points $\{h_i\}$, $i = 1, N$. The algorithm proceeds by returning to step 2.

The two sources of error in this procedure are in the numerical integration of the differential equations and in the interpolation. The error of numerical integration can be controlled by taking smaller step sizes in the integration. The error in interpolation occurs both in the determination of Ψ and in constructing $G(h, t + \Delta t)$ from the tabular function $\{h_i, G_i\}$. This error can be controlled by increasing the number of differential equations which are solved, i.e., decreasing h_i or by strategically locating the h_i. For the calculations reported here the time step was 2 days. The partition points were $h_1 = 0$ cm, $h_i = 10 \times 2^{i-1}$, $i = 2, 10$.

Calculated response. The thickness distribution equation was integrated numerically over a 2-year period. At the end of the period the calculated distribution, shown in Figure 12*b*, was quite similar to the typical observed distributions, shown in Figure 3. From this comparison we conclude that the model is qualitatively realistic. The 2-year history of the thickness distribution is portrayed in Figure 13. The high-frequency variations in $g(h)$, with periods of 1 week to 1 month, are forced by the deformation.

The major variation in the thickness distribution is due to the annual thermodynamic cycle. Each year, late in June, the onset of melting triggers a rapid change in the thickness distribution, most noticeable in the ice thinner than about 1 m. All ice thinner than about 60 cm in June will have vanished into open water by mid-August. In both summers the area of open water (represented in the calculations as ice thinner than 10 cm) grew to about 15% (Figure 12*c*), which is in agreement with summer submarine observations reported by *Wittmann and Schule* [1966]. At the end of the first summer a strong convergent event closed up the open water, whereas after the second summer the area of open water was frozen and ridged into the next thicker categories of ice.

Ice of intermediate thickness, say, 160–640 cm, is almost unchanged at the end of the 2-year period; it accounts for 68% of the total area at the beginning and 69% at the end.

The amount of very thick ice is seen in Figure 13 to decrease throughout the calculation because of melting, the generally divergent trend, and the inability of our weighting function

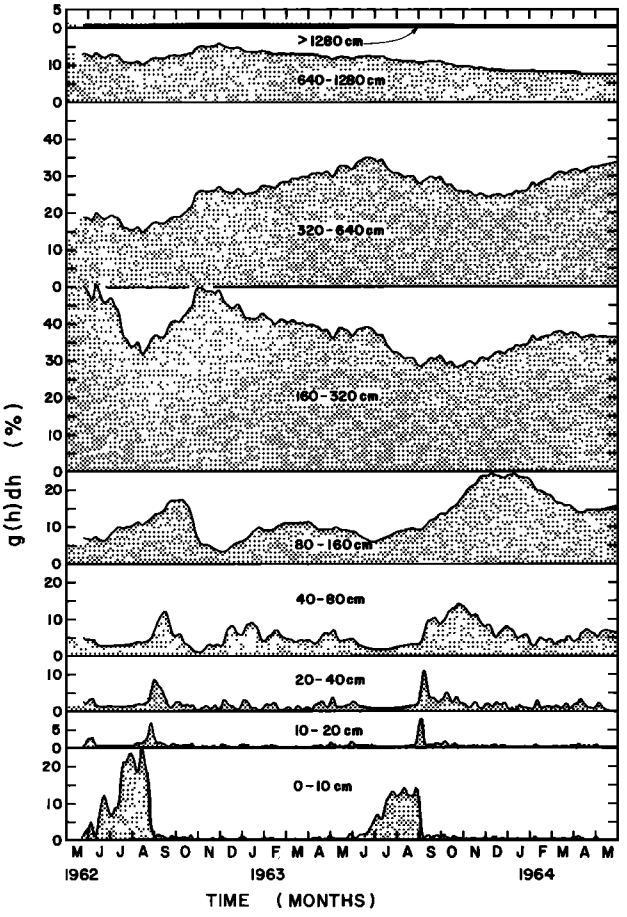

Fig. 13. The 2-year history of the thickness distribution, using the initial condition shown in Figure 12*a*.

and ridging multiplier ($k = 5$) to produce sufficiently thick ice. Figure 14 shows that the thickest ice produced ($5h^*$) was seldom thicker than 9 m in the winter of 1962–1963 and never even reached 640 cm the following winter. We cannot make any comparison with observed ridge counts because our formalism does not treat individual features, nor is there any simple relation between ice thickness and ridge geometry.

The mean thickness $\bar{h}$ was 368 cm initially and decreased to 345 cm over the 2 years (Figure 14). Referring to (13), we see that changes in $\bar{h}$ are only due to thermodynamics and to the flux of ice into the region; ψ, conserving volume, cannot alter $\bar{h}$. The observation that $\bar{h}$ does not change greatly implies that the thermodynamic production of ice is approximately balanced by the generally divergent motion of the pack. The rate of mass production $\bar{f}$, which approximately balances $-h$ div v, fluctuates between 0.25 and 0.75 cm d^{-1} from September to May and then drops to a minimum of about -1.2 cm d^{-1} in July. Figure 15 shows no autumn maximum in $\bar{f}$ because even though there is a large percentage of open water and thin ice, the value of $f(h = 0)$ is still well below its winter maximum.

The strength p^*, being an integral over only the thin end of the thickness distribution, is much more variable than $\bar{h}$, as Figure 16 illustrates. In fact, because of our arbitrary assumption that G^* is 15%, an amount of 15% open water causes the integral in (14) to evaluate to zero. This accounts for the dramatic effect of the summer melt on p^*. While the extreme weakening of the pack each summer is a thermodynamic effect, the deformation can cause considerable strengthening, as happened in the fall of 1962, and is responsible for the fluctuating strength during the winter. Deformations over periods of a week or 2 are of the order of 1–5%, and the calculated fluctuations in p^*, though not enormous, can exceed 100%. One can see from Figure 16 that, as expected, changes in p^* are out of phase with area changes. The increased proportion of thin ice produced by divergence reduces p^*. Convergence removes thin ice, increasing the resistance to further compression.

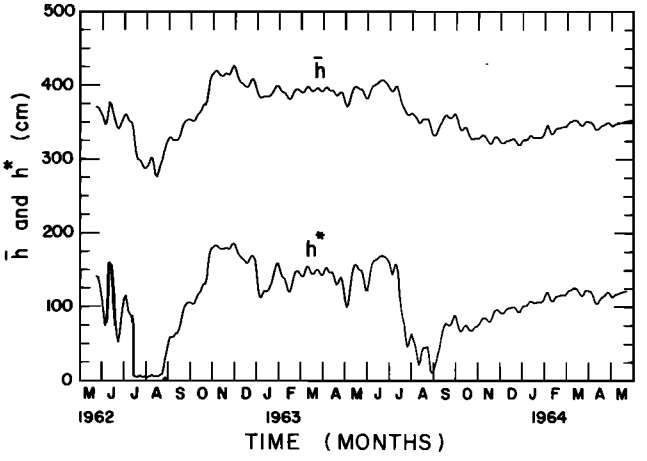

Fig. 14. Mean thickness $\bar{h}$ and thickness h^* versus time, beginning with the initial condition in Figure 12*a*.

For comparison, a run was made starting from an initial condition with all the ice between 0 and 20 cm, using the same growth rates for f and the same strain rates to construct ψ and div v. The growth rates probably apply quite reasonably to an arctic ocean covered by very thin ice, but the deformations in such an ice cover would surely have been much greater than those used here, which, unfortunately, are all we have. The time history of $g(h)$ is shown in Figure 17. In this case the thermodynamic and divergence terms do not balance; because of the larger area of thin ice, ice production is rapid, while the volume of ice exported by the divergence term is small. The net effect after 2 years is to produce a mean thickness of 246 cm and a distribution that is similar to the observed distributions, except in the very thick ice (Figure 12*d*). The strength p^* converges to within 10% of that of the previous case as early as January 1963, illustrating that the thin end of the distribution, to which p^* is sensitive, adjusts more quickly than the thicker end. We take these results to suggest that the ice pack, as characterized by its thickness distribution, is in a near-equilibrium state.

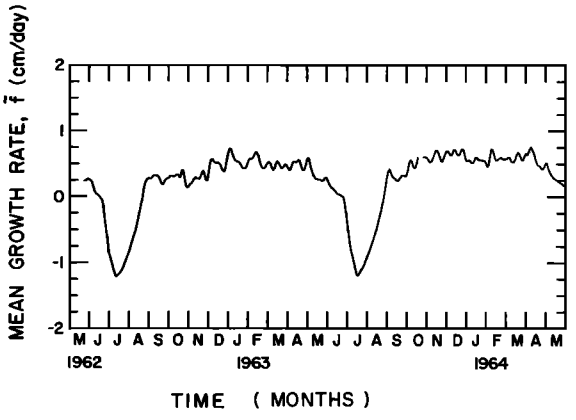

Fig. 15. Mean growth rate $\bar{f}$ versus time, for the initial condition in Figure 12*a*.

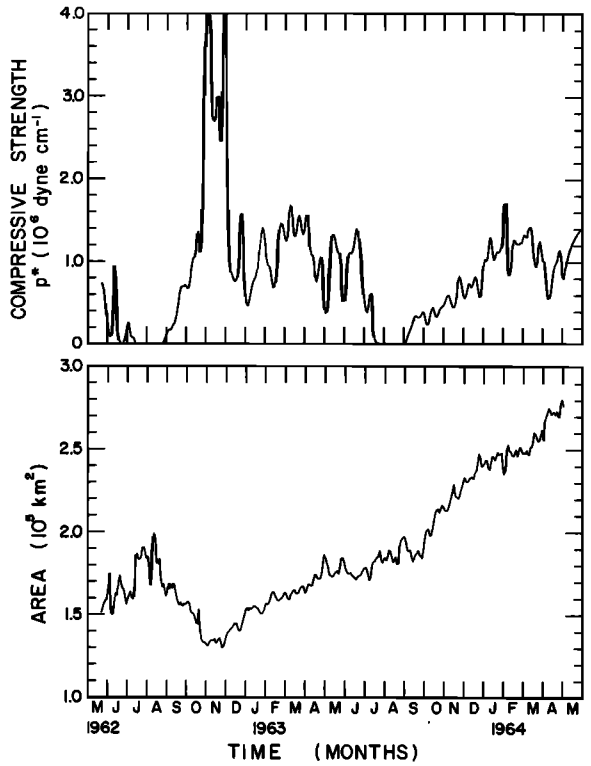

Fig. 16. The temporal behavior of p^* and of the area of the triangle formed by the three drifting stations.

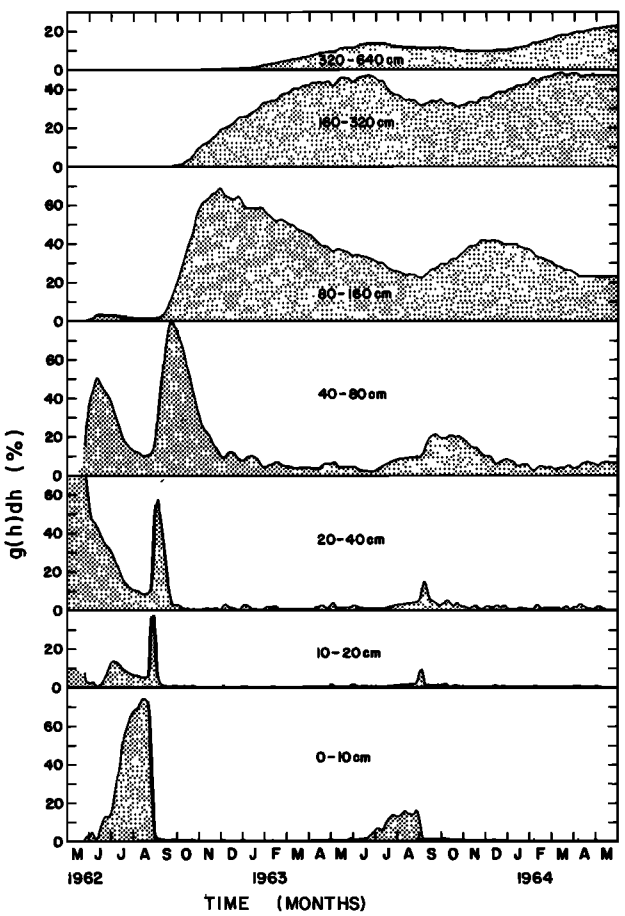

Fig. 17. The 2-year history of the thickness distribution starting from an initial condition of no ice thicker than 20 cm. Ice thicker than 640 cm was never produced during the period.

Sensitivity to the redistributor. The major uncertainty in the model is the precise form of the redistributor ψ. We must ask therefore whether the results of model calculations are dominated by the physics which we have modeled properly in the thermodynamic term and the divergence term or whether they are dominated by the uncertainties in the form of ψ. Parameter studies have been made, using the limits of reasonable values for the weighting function b and for the ridging multiplier k.

By changing the shape of b we can involve a greater or smaller proportion of the thinnest ice in the redistribution process. The effects of changing the form of b are quite mild. Changes in the mean thickness between the extreme cases, for instance, amount to about 10% after 2 years. The strength p^* is somewhat more sensitive, differing about 50% between extreme cases. Since the strength depends largely on the area of thin ice, a weighting function that consumes more of the thinnest ice produces a stronger ice pack.

Modifying k from the value of 5, taken as standard, to extremes of 2 (simple rafting) and 10 has an effect on p^* of several hundred percent. The reason for this is that larger values of k imply thicker ridges which, because of their greater potential energy, require more work to build and hence offer a greater resistance p^*.

The scale of p^*, then, is significantly affected by assumptions in ψ. Nevertheless, its behavior, whether it is increasing or decreasing, and the relative size of different events, appears, on the basis of this study, to be insensitive to those assumptions.

Discussion

In this paper we have addressed only one of several important questions that must be solved before the interactions between sea ice and its environment can be understood. We have presumed the growth rates and deformations of the ice to be given and asked, how do these change the state of the ice pack as characterized by its thickness distribution? In a more complete model of the pack ice the inputs to the thickness distribution equation would come from energy balance and heat conduction equations to give growth rates and a momentum balance and mechanical constitutive equations to give the ice deformation. The principal coupling between these equations is in the compressive strength p^* which, through the constitutive law, regulates the ice pack's ability to deform.

The present theory suffers from a burdensome and arbitrary redistribution function ψ. Observations are badly needed to identify which parts of the general formulation are necessary and valid and to replace the guesswork on which the precise forms of $b(h)$, $\gamma(h_1, h_2)$, and $\alpha_0(\theta)$ were based. Data collected during the Arctic Ice Dynamic Joint Experiment in 1975–1976 should be useful for this purpose.

In the broader context of climate modeling the ice pack is important because it controls the heat and momentum exchange between the atmosphere and the ocean. The important parameters appear to be the position of the ice boundary, the areas of open water and very thin ice, and the ice roughness. While work on including an active ice pack in climate models is just beginning, it is probable that the notion of an ice thickness distribution will be of value.

Acknowledgments. We would like to acknowledge the assistance of all our colleagues at Aidjex, with special thanks to John Nye, whose comments have helped us to clarify the essential ideas and to avoid entanglement in the less essential details. This work was supported by the National Science Foundation under grant OPP71-04031 (formerly GV-28807) and by the Office of Naval Research, Arctic Program, un-

der contract N00014-67-A-0103-0007. Contribution 339, Department of Atmospheric Sciences, University of Washington, Seattle, Washington 98195.

REFERENCES

Andersen, D. L., Growth rate of sea ice, *J. Glaciol., 3,* 1170–1172, 1961.

Badgley, F. I., Heat balance at the surface of the Arctic Ocean, Proceedings of the Symposium on the Arctic Heat Budget and Atmospheric Circulation, *RM-5233-NSF,* edited by J. O. Fletcher, pp. 267–278, Rand Corp., Santa Monica, Calif., 1966.

Coon, M. D., G. A. Maykut, R. S. Pritchard, D. A. Rothrock, and A. S. Thorndike, Modeling the pack ice as an elastic-plastic material, *Aidjex Bull., 24,* 1–105, 1974. (Also published as *PB 232 231/AS,* Nat. Tech. Inform. Serv., Springfield, Va.)

Hibler, W. D., III, W. F. Weeks, A. Kovacs, and S. F. Ackley, Differential sea ice drift, 1, Spatial and temporal variations in sea ice deformation, *J. Glaciol., 13,* 437–456, 1974.

Hildebrand, F. B., *Advanced Calculus for Applications,* p. 102, Prentice Hall, Englewood Cliffs, N. J., 1962.

LeSchack, L. A., W. D. Hibler III, and F. H. Morse, Automatic processing of arctic pack ice data obtained by means of submarine sonár and other remote sensing techniques, Propagation Limitations in Remote Sensing, *AGARD-CP-90-71,* edited by J. B. Lomax, pp. 5-1–5-14, N. Atl. Treaty Organ., Brussels, 1971.

Maykut, G. A., and N. Untersteiner, Some results from a time-dependent, thermodynamic model of sea ice, *J. Geophys. Res., 76,* 1550–1575, 1971.

Parmerter, R. R., and M. D. Coon, Model of pressure ridge formation in sea ice, *J. Geophys. Res., 77,* 6565–6575, 1972.

Rothrock, D. A., The energetics of the plastic deformation of pack ice by ridging, *J. Geophys. Res., 80,* this issue, 1975.

Swithinbank, C., Arctic pack ice from below, in *Sea Ice: Proceedings of an International Conference, Reykjavik, Iceland,* edited by T. Karlsson, pp. 246–254, National Research Council, Reykjavik, 1972.

Thorndike, A. S., Strain calculations using Aidjex 1972 position data, *Aidjex Bull., 24,* 107–129, 1974. (Also published as *PB 232 231/AS,* Nat. Tech. Inform. Serv., Springfield, Va.)

Thorndike, A. S., and G. A. Maykut, On the thickness distribution of sea ice, *Aidjex Bull., 21,* 31–48, 1973. (Also published as *PB 223 387,* Nat. Tech. Inform. Serv., Springfield, Va.)

Wittmann, W. I., and J. J. Schule, Comments on the mass budget of arctic pack ice, Proceedings of the Symposium on the Arctic Heat Budget and Atmospheric Circulation, *RM-5233-NSF,* edited by J. O. Fletcher, pp. 215–246, Rand Corp., Santa Monica, Calif., 1966.

(Received April 1, 1975;
revised June 19, 1975;
accepted June 19, 1975.)